Intramolecular S··O Chalcogen Bond as Stabilizing Factor
in Geometry of Substituted Phenyl-SF$_3$ Molecules

Vincent de Paul N. Nziko and Steve Scheiner*

Department of Chemistry and Biochemistry

Utah State University

Logan, UT 84322-0300

ABSTRACT

Density functional methods are used to examine the geometries and energetics of molecules containing a phenyl ring joined to the trigonal bipyramidal SF$_3$ framework. The phenyl ring has a strong preference for an equatorial position. This preference remains when one or two ether -CH$_2$OCH$_3$ groups are added to the phenyl ring, *ortho* to SF$_3$, wherein an apical structure lies nearly 30 kcal/mol higher in energy. Whether equatorial or apical, the molecule is stabilized by a S··O chalcogen bond, sometimes augmented by CH··F or CH··O H-bonds. The strength of the intramolecular S··O bond is estimated to lie in the range between 3 and 6 kcal/mol. A secondary effect of the S··O chalcogen bond is elongation of the S-F bonds. Solvation of the molecule strengthens the S··O interaction. Addition of substituents to the phenyl ring has only modest effects upon the S··O bond strength. A strengthening arises when an electron-withdrawing substituent is placed *ortho* to the ether and *meta* to SF$_3$, while electron-releasing species produce an opposite effect.

*steve.scheiner@usu.edu

Keywords: CH··F H-bond, NBO, electron density shift, isodesmic

INTRODUCTION

Fluorine-containing compounds are of great importance in organic synthesis, and in the pharmaceutical and agro-industries. Fluorinated compounds constitute about 25% of pharmaceutical and 30% of all agricultural compounds [1-4]. Glycosyl fluorides have been widely and effectively used for purposes of *O-* and *C-*glycosylation. The addition of a fluorine atom to a molecule can have a variety of dramatic effects on its properties, making it more selective, increasing its efficacy, or making it easier to administer [2, 5-7].

The preparation of fluorinated compounds made use of SF_4 in order to convert alcohols, aldehydes, ketones and carboxylic acids to their respective fluorinated forms [8]. Due to the highly toxic and gaseous nature of SF_4, other fluorinating agents with improved physical and chemical behavior were highly sought after. In the 1970s, SF_4 was largely replaced by dialyklaminosulfur trifluorides. One of these, diethylaminosulfur trifluoride (DAST illustrated in Scheme Ia) was effective [9] for deoxofluorination of alcohols and C=O containing molecules. A major drawback, however, was the thermal instability of DAST, coupled with its inability to fluorinate certain ketones. These problems have led to a number of other deoxofluorinating agents, such as deoxofluor (Scheme Ib) [10] and Yarovenko and Ishikawa reagents [11-12], but each of these have been limited in terms of molecules they can easily fluorinate.
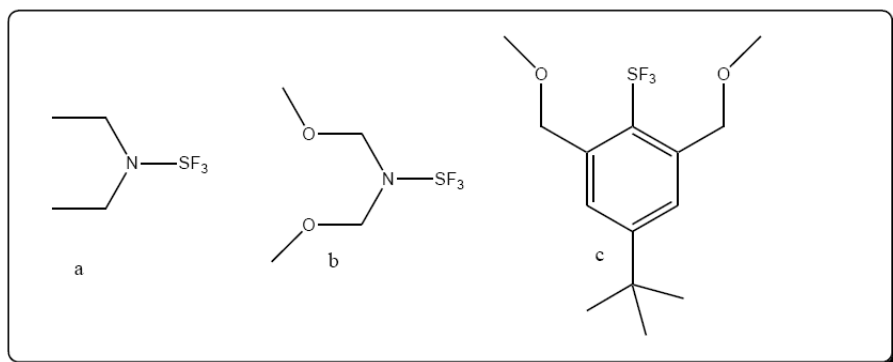

Figure 1. Structure of a. DAST b. Deoxofluor c. 4-tert-butyl-2,6-bis(methoxy-methyl)sulfur trifluoride

In 2010, Umemoto et al [13] reported a series of aryl fluorinated compounds with improved reactivity as deoxofluorinating agents, with high thermal stability that led to extensive applications. They suggested that the improved thermal stability of phenylsulfur trifluorides probably resulted from strong C-S bonds, compared to the weak N-S bonds in DAST and deoxofluor. A series of related compounds were tested for their efficacy, and some of the most promising molecules contained one or more ether groups bound to the phenyl, in positions adjacent to the SF_3 group, as for example in Scheme Ic. There was limited structural information available about these molecules, but ^{19}F and ^{1}H NMR data strongly suggested a trigonal bipyramidal geometry around the

sulfur atom. The authors suggested that the stability of this series of molecules might be due in part to coordination of electron-donating ether oxygen atoms to the electron-deficient SF_3 group.

The potential of this sort of molecule as a deoxofluorinating agent leads to the necessity for better understanding of the underlying factors that make it so effective. This information ought to lead to a rational means of designing and synthesizing new systems with superior effectiveness. From a more basic perspective, there is little known about the chalcogen S··O bond that has been proposed as a key ingredient in the efficacy and thermal stability of these systems. Even as information begins to accumulate about such chalcogen bonds [14-30], most of this work has been aimed toward intermolecular interactions, not the sort of intramolecular bonds that are characteristic of these systems. Unlike the former, the intramolecular sort of S··O bonds are saddled with a variety of inescapable geometrical restrictions that are part and parcel of each molecule. Another distinguishing feature of intramolecular bonds is the strong interdependence of the electronic structure around the sulfur and oxygen atoms, which are connected by only a few covalent bonds between them.

There are a number of very important issues related to this series of molecules, their geometry, and their potential as fluorinating agents. Are there in fact intramolecular O··S contacts present in these systems? How strong are these noncovalent bonds, and do they persist in different solvents? How does the presence of one such S··O contact affect the properties of a second? Importantly, what are the effects of these interactions upon the neighboring S-F bonds which are the source of the fluorine atoms during the fluorination process? How are the structure and properties affected by the presence of various substituents on the aromatic ring, and in different positions?

A straightforward means to address these important questions is via quantum chemical calculations. In this work, the molecules of interest have been built and studied in stages. First the intrinsic geometric preferences of an unsubstituted phenyl-SF_3 molecule are examined. We determine first whether this molecule adopts a trigonal bipyramidal geometry as is the case in the catalysts of interest, and if so what is the difference in energy between an apical or equatorial placement of the phenyl group. An ether functionality is then added to the phenyl ring, as in the molecules under study. Careful examination determines whether there is indeed a S··O chalcogen bond present, and if so, how stable is this structure in comparison to other geometries. The possibility of H-bonds (HBs) of the CH··F type influencing the structure is examined as well. The system is brought into exact correspondence with the deoxofluorinating agents of interest when a second ether group is added. (The -CH_2OCH_3 group used here corresponds to the functionality that showed the highest percent yield in the experimental work [13].) Is there a S··O chalcogen bond present here also, and if so, might there be a second as well? In terms of rationally designing a more effective agent, the first step might be to add a substituent to the phenyl ring. A set of different substituents are therefore added, both electron-withdrawing and releasing. And these substituents are added to various positions on the phenyl ring to determine which

3

would be most effective. And finally, the molecules are examined not only *in vacuo* which tells much about their intrinsic properties, but also in solution where they would normally be used.

METHODS

Molecular systems were examined using the B3LYP variant of density functional theory, and the aug-cc-pVDZ basis set. Calculations were carried out using the Gaussian-09 package [31] of codes. Solvent was introduced via the PCM method [32]. Second-order interaction energies between molecular segments were computed using the Natural Bond Orbital (NBO) approach [33-34], as implemented in Gaussian. Atoms in Molecules (AIM) methodology [35] was used to analyze the electron density of the system using the AIMALL [36] program.

RESULTS AND DISCUSSION

When one fluorine atom of SF_4 is replaced by a phenyl group, there is only one minimum on the monosubstituted molecule's potential energy surface. As seen in Fig 1, the phenyl group of 1A assumes an equatorial position, wherein two of its CH groups are in near proximity to the apical fluorine atoms, with r(H··F) less than 2.3 Å. The optimization of this same molecule, with the phenyl group placed in an apical position decayed to the equatorial conformer 1A.
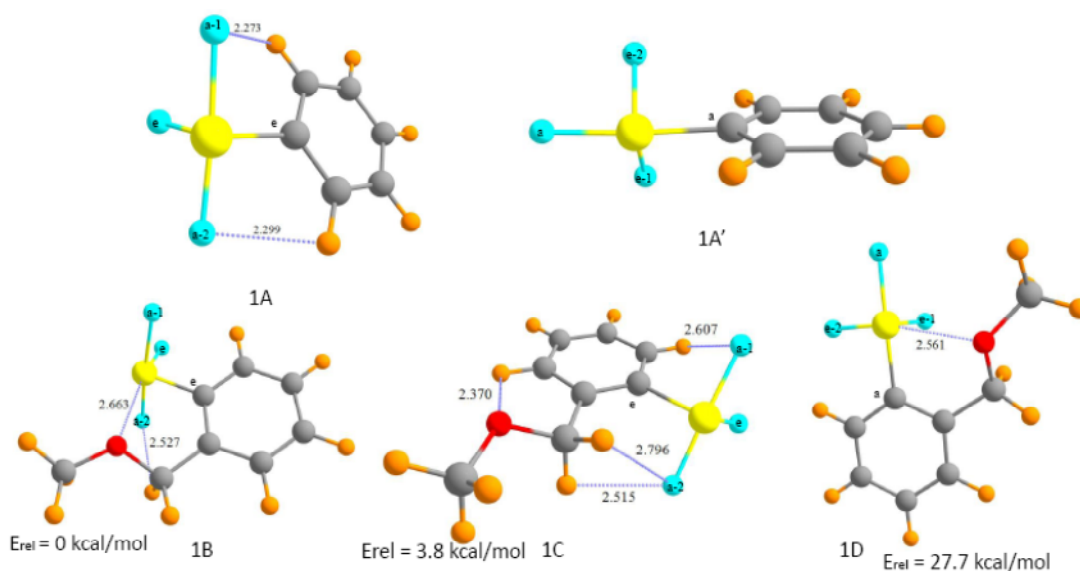

Fig 1. Optimized geometries of various minima. Distances in Å.

The situation changes to a certain extent when an *ortho*-H atom of the phenyl group is replaced by a -CH_2OCH_3 ether group. There are now two equatorial arrangements that occur as minima. The more stable of the two is displayed as 1B in Fig 1, and contains a close approach of the ether oxygen to the sulfur atom, with R(S··O)=2.663 Å. There is also a fairly close approach of an apical fluorine atom to a methylene proton, 2.527 Å. The stabilizing O··S chalcogen bond is replaced by several CH··F H-bonds and one CH··O in the other

4

equatorial configuration 1C. But these HBs cannot compensate for the loss of the O··S chalcogen bond, making this structure less stable than 1B by 3.8 kcal/mol.

As is indicated in Fig 1, and as is true for all of the structures described here, the geometry around the sulfur atom fits the description of a "see-saw", i.e. a trigonal bipyramid with one of the equatorial sites occupied by a S lone pair. As is typical of these sorts of geometries, the bulging lone pair squeezes the bonding pairs closer together than would be the case in a full trigonal bipyramid of bonding pairs. The angles between each pair of apical S-F/C bonds were found to be within 10° of the classical 180°, and angles between apical and equatorial bonds are within 6° of the unstrained 90°. The greatest strain induced by the lone pair occurs within each pair of equatorial bond pairs, so these angles lie in the range 95-106°, smaller than the unstrained value of 120°. Noncovalent S··O chalcogen bonds occur when charge is transferred from the oxygen atom to the σ*(S-F) antibonding orbital which lies directly opposite the associated FH covalent bond. They do not represent a fifth covalent bond around the S which would alter its overall geometry. Nor is the formation of a chalcogen (or pnicogen or halogen) bond impeded by the presence of one or more lone pairs on the central atom in the general direction [37-48] of the noncovalent bond. The equatorial SF bonds have associated with them a vacant position which may be occupied by a S··O chalcogen bond. In contrast, such noncovalent bonds are not possible opposite an apical SF bond, since this position is already occupied by a second apical covalent bond.

The presence of the introduced ether group also results in the appearance of a minimum on the surface in which the substituted phenyl group occupies an apical position, albeit 27.7 kcal/mol higher in energy than the global minimum 1B. Like the latter, this apical minimum 1D also contains a close approach of the oxygen and sulfur atoms; in this case R(O··S) is 0.1 Å shorter at 2.56 Å. It is likely that it is the presence of this chalcogen bond which permits this configuration to exist as a minimum on the surface, as there is no apical minimum in the absence of the ether. Not only is R(S··O) shorter in 1D than in 1B, but the NBO value of E(2), a measure of charge transfer from the O lone pairs to the σ*(SF) antibonding orbitals, is 10.81 kcal/mol in 1D, even larger than in 1B where it is 6.66 kcal/mol.

Addition of a second ether functionality to the other *ortho* position of the phenyl group imparts a more complicated character to the potential energy surface. There is still a heavy preference for equatorial placement of the phenyl. The global minimum 2A in Fig 2 is stabilized by three attractive interactions. One ether oxygen atom participates in a O··S chalcogen bond with the sulfur atom, with R(O··S)=2.626 Å. A methylene H comes within 2.426 Å of an apical fluorine atom. Without a second site on S available for another O··S chalcogen bond, the other ether O associates instead with a phenyl H, forming a strong CH··O HB, with R(H··O) as short as 2.226 Å. The second equatorial minimum 2B is less stable by 2.2 kcal/mol, and relies for its stability on HBs alone, of both the CH··O and CH··F varieties, some as short as 2.3 Å. Again, these HBs are unable to make this structure as stable as the one containing the chalcogen bond.
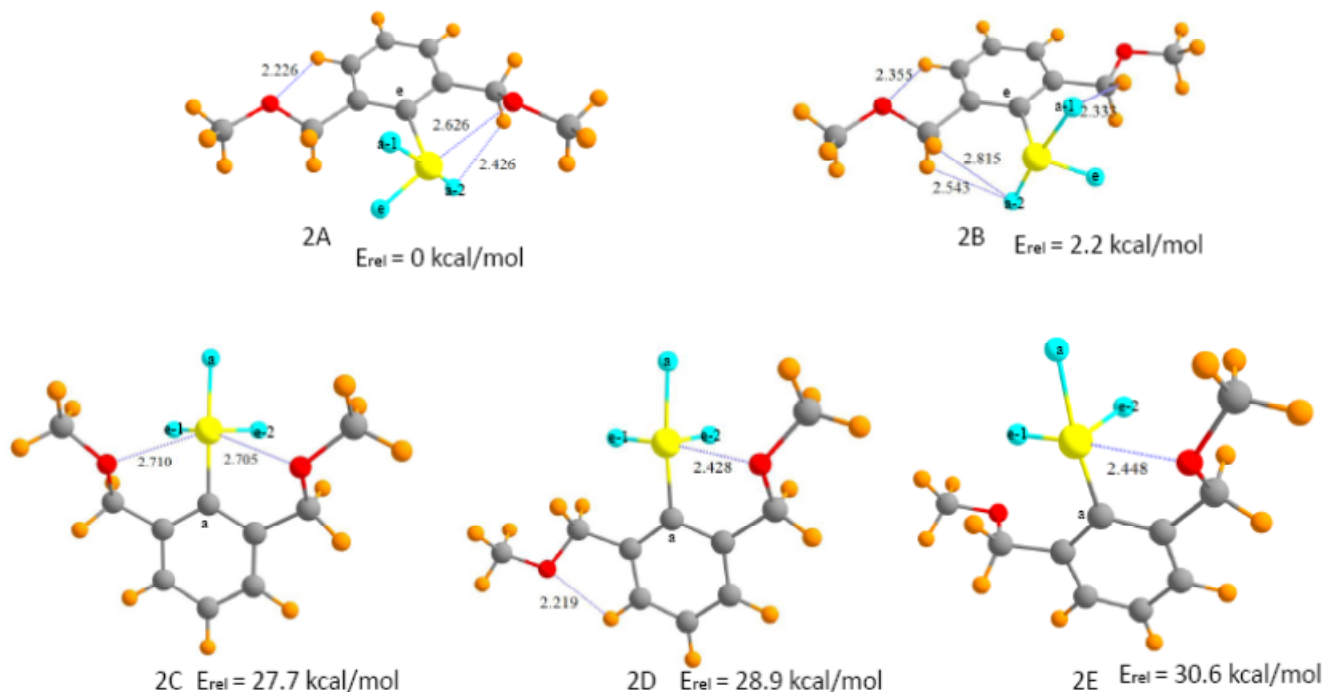
Fig 2. Optimized geometries of various minima of molecules containing two -CH$_2$OCH$_3$ groups. Distances in Å.

Apical positioning of the phenyl group again results in a much less stable set of minima, 28-31 kcal/mol higher in energy than the equatorial global minimum. The apical placement of the substituent opens up a second site opposite a S-F$_e$ bond which might be occupied by a second O··S chalcogen bond. And indeed, two such bonds are observed in the most stable of the apical conformers 2C. Reducing this number of chalcogen bonds to one raises the energy in 2D and 2E, even in the presence of a CH··O HB in 2D. Comparison of 2C with 2D and 2E indicates a negative cooperativity in the two S··O chalcogen bonds. R(S··O) is longer in 2C by nearly 0.3 Å, and the two values of E(2) are 6.5 kcal/mol in each of the S··O bonds of 2C, smaller than 17.81 of 2D or 16.41 kcal/mol of 2E.

One can conclude that a phenyl substituent has a strong propensity to occupy an equatorial position around S. If the phenyl also contains one or more ether linkages, the oxygen atoms are drawn to form a O··S chalcogen bond which will be present in the global minimum in all cases. This bond can stabilize an apical substitution to the point of becoming a true minimum, even if nearly 30 kcal/mol higher in energy than equatorial. This apical placement opens up a second site for S··O chalcogen bond formation, which is indeed occupied in the disubstituted molecule 2C. These S··O chalcogen bonds prove a stronger influence upon conformation than even short CH··O or CH··F HBs.

Solvation Effects

As some of the most useful behavior of these molecules occurs in solution, it is worthwhile to examine how solvation affects their properties. Table 1 focuses on those structures that contain a S··O chalcogen bond, e.g. 1B and 1D. The data in the leftmost section of Table 1 shows that the introduction of solvent causes a slight lowering of the energies of the secondary minima relative to the global minimum. For example, the energy of 1D relative to 1B drops from 27.7 kcal/mol in the gas phase to 25.0 kcal/mol in dichloromethane (DCM: $\varepsilon=8.9$), and then to 23.8 kcal/mol in water ($\varepsilon=78$). Similar reductions are noted for the 2C, 2D, 2E series relative to 2A. It would appear then that solvent allows a mild stabilization of apical geometries in comparison to the more stable equatorial structures.

Table 1. Relative energies, O···S interatomic distances, and interaction angle in configurations containing a S··O bond.

	E_{rel}, kcal/mol			R(O··S), Å			θ(O··SF), degs		
	Gas	DCM	Water	Gas	DCM	Water	Gas	DCM	Water
1B	0	0	0	2.663	2.556	2.529	165.0	172.5	173.4
1D	27.7	25.0	23.8	2.561	2.370	2.317	167.6	172.0	173.1
2A	0	0	0	2.626	2.551	2.532	172.0	174.4	174.8
2C	27.7	23.3	21.7	2.710	2.583	2.529	157.4	159.7	160.8
2D	28.9	25.4	24.2	2.428	2.295	2.254	171.5	172.2	172.3
2E	30.6	26.2	24.7	2.448	2.322	2.278	171.0	171.7	172.0

The next section of Table 1 shows that the R(O··S) distances of the chalcogen bonds undergo a contraction as solvent is introduced and becomes more polar. For example, the first row of Table 1 shows that the R(O··S) distance in 1B is 2.663 Å *in vacuo*, contracts to 2.556 Å in dichloromethane, and then to 2.529 Å in water. This contraction is even stronger in the apical configuration 1D, where water reduces this distance by 0.24 Å. Other rows in Table 1 show that the reduction occurs not only when there is a single S··O chalcogen bond, but also in 2C where there are two such bonds, both contracted by 0.18 Å when immersed in water. Note that the solvent-induced bond contractions are of larger magnitude in the apical structures in comparison to the equatorial, consistent with the energetic trends in Table 1. Another sign of growing strength of these S··O noncovalent bonds in solution arises by examination of the θ(O··SF) angles which all become more linear. Again taking 1B as an example, this angle is raised from 165° in the gas phase to 173° in water.

One can also consider the NBO second order perturbation energy E(2) associated with charge transfer from the O lone pairs to the σ*(SF) antibonding orbital as a measure of chalcogen bond strength. These values in the various solvation situations are reported in Table 2. The major component refers to the SF bond that lies directly opposite the O, whereas a smaller value is associated with the σ* antibonding orbital of the other equatorial SF bond. (This secondary transfer was shown to be important in our earlier study [49] of the interaction of SF_4 with several amines.) 1B and 2A are exceptions since the second equatorial position is taken up not by an F but rather by the phenyl group, so there is no minor component. The important finding in Table 2 is that the increasing polarity of the solvent raises E(2), consistent with the trends in the energetic and geometrical data in Table 1.

Table 2. NBO E(2) (kcal/mol) for transfer from O lone pairs to σ*(SF) antibonding orbital.

	gas		DCM		water	
	Major[a]	Minor[b]	Major	Minor	major	Minor
1B	6.66	-	9.71	-	10.67	-
1D	9.67	1.14	17.76	2.25	20.80	2.68
2A	8.35	-	9.98	-	10.69	-
2C	6.24	6.20	10.21	10.21	12.42	12.42
2D	17.59	3.58	23.19	3.97	25.73	4.48
2E	16.14	3.34	20.98	3.62	23.96	4.16

[a] SF bond directly opposite O
[b] other equatorial SF bond

Internal Bond Perturbations

Prior work with the SF_4 molecule [49] has shown that its participation in a chalcogen bond tends to lengthen all of its S-F bonds, albeit in the context of an intermolecular interaction. It was therefore of interest to examine whether the same trend occurs in the case of an intramolecular chalcogen bond. The optimized geometry of 1A was taken as the reference point for an equatorial phenyl group, but without any possibility of a S··O chalcogen bond. As indicated earlier, there is no corresponding apical minimum on the surface of this system in the gas phase. In order to construct such a reference structure, a restraint was introduced into the molecule, wherein $\theta(C-S-F_a)$ was held constant at 177.3°, the angle which is adopted by the apical minimum in DCM solvent. This structure is illustrated as 1A' in Fig 1.

The left side of Table 3 contains the changes in the r(SF) bond lengths relative to equatorial 1A whereas the apical structure 1A' was taken as the reference for molecules on the right side of the Table. Considering 1B

first, this molecule contains a O··S chalcogen bond which stretches the S-F_e bond which lies directly opposite the incoming oxygen atom, by 4.4 mÅ. One of the apical S-F bonds is stretched by 6 mÅ, but the longest stretch of 20 mÅ is associated with F_{a2} which engages in a CH··F HB with a methylene proton. The pattern of a small stretch for the S-F_e and longer stretches for the apical S-F bonds is repeated in 2A, which also contains a noncovalent S··O bond. Neither 1C nor 2B contain such a chalcogen bond, and in both of these cases S-F_e suffers a contraction rather than a stretch. One of the S-F_a bonds shows little change, and the other such bond undergoes a small stretch. Thus, the S-F bond elongations associated with O··S chalcogen bond formation are either absent or much reduced in the absence of such a bond.

Table 3. Changes in r(S-F) bond lengths (mÅ) of indicated molecules.

	Equatorial[a]					Apical[b]			
				vacuum					
	1B	1C[c]	2A	2B[c]		1D	2C	2D	2E
e	4.4	-5.0	5.8	-4.8	e-1	8.0	-3.6	7.1	5.0
a-1	6.0	-0.5	10.6	1.6	e-2	-3.4	-3.6	-4.0	-11.7
a-2	20.5	4.5	22.3	5.4	a	40.0	66.8	64.2	62.0
				DCM					
e	7.8	-8.0	6.5	-9.4	e-1	3.82	0.22	5.63	0.63
a-1	19.3	-0.2	19.2	2.5	e-2	4.20	0.22	7.64	3.85
a-2	19.3	3.9	21.3	5.1	a	119.5	156.2	135. 6	125.8
				Water					
e	9.3	-8.3	7.3	-10.1	e-1	5.4	4.7	6.5	5.8
a-1	23.4	1.2	22.6	3.2	e-2	9.9	4.7	14.5	7.9
a-2	18.5	3.2	20.0	4.1	a	158.5	208.6	170.0	156.1

[a]relative to 1A
[b]relative to apical geometry 1A'
[c]no S··O bond present

Turning to the molecules in which the phenyl group occupies an apical position, the S··O chalcogen bond in 1D has small but opposite effects on the two S-F_e bonds, one stretching and the other contracting. It is the apical S-F bond that undergoes the largest change, stretching by 40 mÅ. This same pattern repeats in the other apical conformations 2C, 2D, and 2E, where the apical S-F bond stretches by a large amount upon formation of the S··O chalcogen bond, between 62 and 67 mÅ. Also common in these structures, the S-F_e bonds undergo much smaller changes in length.

Perusal of data in the lower portions of Table 3 indicates a repeat of the patterns found within the gas phase for the most part, although these stretches generally increase in solution. For example, the S-F_e bond stretch in 1B increases from 4.4 mÅ in the gas phase, to 7.8 in DCM and then to 9.3 mÅ in water. These solvent-induced

enhancements are most noticeable in the stretches of the S-F$_a$ bond in the apical conformations. Elongations of 40 to 67 mÅ in the gas phase are magnified several-fold to as much as 209 mÅ in water.

One might anticipate that S-F bond elongations would be tied to bond polarization making these fluorine atoms more negative. The changes in the NBO charges on the fluorine atoms reported in Table 4 indeed confirm this expectation. For example, the greater stretches of the apical S-F bonds in 1B, compared to equatorial, are consistent with the greater increase of F$_a$ negative charge. And in those cases where a S-F bond contraction is noted, e.g. 1C and 2B, the fluorine atoms become more positive. Just as the longest S-F bond stretches occur in the apical bond in aqueous phase on the lower right of Table 3, so too does the F$_a$ atom gain the largest negative charge in Table 4.

Table 4. Changes in NBO atomic charges (me) of F atoms of indicated molecules.

	Equatorial[a]				Apical[b]				
	1B	1C[c]	2A	2B[c]		1D	2C	2D	2E
vacuum									
e	-0.6	5.2	-0.9	4.5	e-1	-4.8	-7.4	-12.8	-5.3
a-1	-9.7	3.3	-11.2	4.8	e-2	-0.9	-7.4	4.7	-3.3
a-2	-14.5	-3.5	-14.4	0.2	a	-29.3	-56.7	-47.9	-47.4
DCM									
e	-3.3	3.4	-3.0	2.7	e-1	-3.6	-12.4	-11.4	-9.3
a-1	-12.2	4.9	-13.1	1.8	e-2	-9.5	-12.4	-18.1	-9.6
a-2	-13.8	-2.4	-14.1	-1.8	a	-57.8	-81.9	-65.6	-62.6
Water									
e	-4.5	1.1	-4.1	2.2	e-1	-3.1	-13.2	-11.0	-9.2
a-1	-12.0	3.2	-14.4	1.6	e-2	-12.1	-13.2	-16.0	-12.0
a-2	-14.8	-2.1	-12.1	-1.8	a	-69.2	-98.5	-75.1	-70.5

[a]relative to 1A
[b]relative to apical geometry 1A'
[c]no S··O bond present

In summary, formation of a S··O chalcogen bond tends to lengthen all of the S-F bonds and to increase the fluorine atom negative charge. The largest effects are associated with the apical S-F bonds. This pattern is observed whether the phenyl substituent is placed in an equatorial or apical position, but the latter results in a much larger S-F$_a$ elongation upon formation of the S··O chalcogen bond. These bond elongations are presumably associated with a weakening which would facilitate the transfer of one or more fluorine atoms during the deoxofluorinating process.

Electron Density Shifts

Another window through which to view the purported formation of an interaction such as a S··O chalcogen bond is via electron density difference maps. The construction of such a map is straightforward in the case of an intermolecular interaction, where it comprises the difference between the density of the complex and the sum of the two isolated subunits of which it is composed. But one cannot do this in the case of an intramolecular interaction where there are no isolated subunits to take as a reference. Instead, the idea of an isodesmic reaction [50]. was used to construct this map. As indicated in Fig 3, C represents the molecule containing the intramolecular interaction of interest between SF_3 and CH_2OCH_3. A and B are both the same as C, but each replaces one of the two functional groups by a simple hydrogen atom. Their sum therefore contains the density of both groups, but without the mutual interaction. The second benzene ring of this sum must be accounted for, so the density of D is added to that of C. The electron density difference map therefore is taken as the sum of (C + D), minus (A + B), which ought to focus on the shifts of density that accompany the formation of the chalcogen bond.
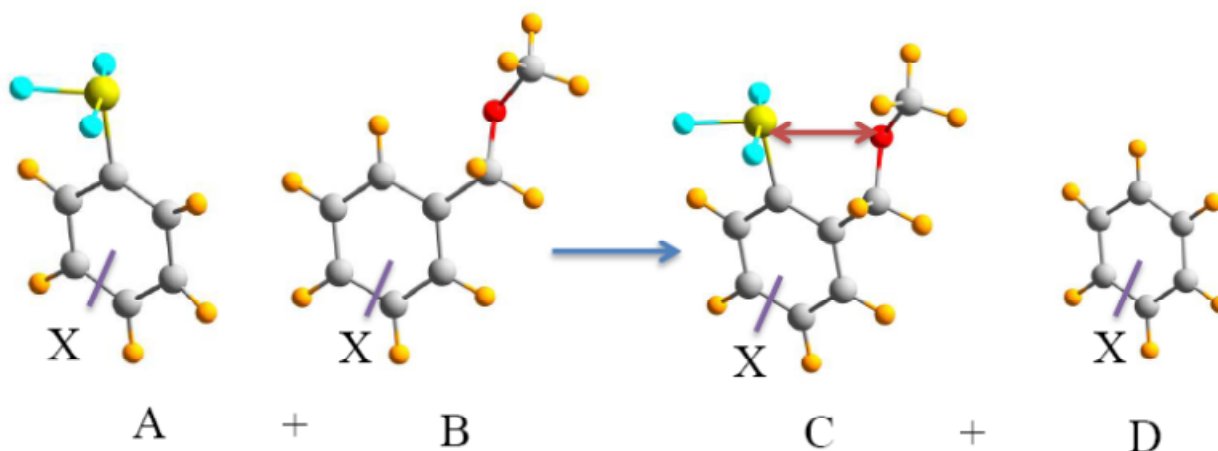

Fig. 3. Molecules used to evaluate density redistribution patterns and isodesmic values of S··O bond energies.

This density shift map is illustrated in Fig 4 where purple and yellow regions respectively indicate gains and losses of density that occur as a result of the formation of the intramolecular S··O noncovalent bond. Perhaps the most important aspect of this figure is the purple buildup of density between the oxygen and sulfur atoms, expected for bond formation. Also noted is a yellow density loss to the immediate left of the sulfur atom, both features that were observed earlier [49] for the intermolecular S··N noncovalent bond between SF_4 and a series of aliphatic and aromatic amines. Another similarity to the intermolecular systems is the buildup of density on the various fluorine atoms, both the one involved in the $O_{lp} \rightarrow \sigma^*(SF)$ charge transfer, and the others as well. It is also worth noting the lack of substantive density rearrangement within the aromatic ring, suggesting its lack of direct involvement in the S··O chalcogen bond.
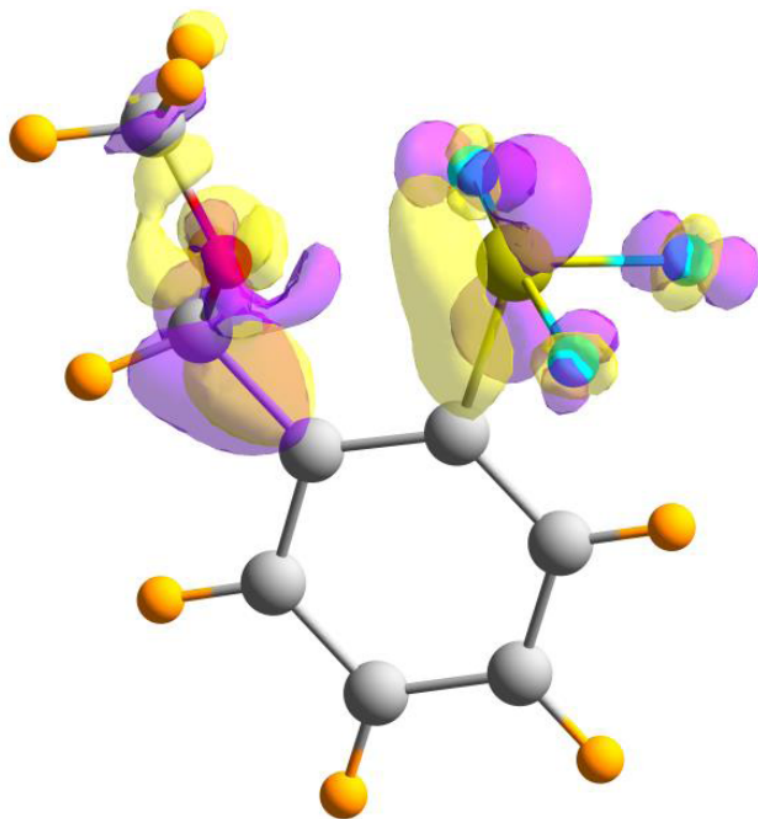
Fig. 4. Electron density redistribution of molecule 1B, using isodesmic system in Fig 3. Purple regions indicate density increase, and losses are shown in yellow. Isocontour illustrated is ±0.0015 au.

Substituent Effects

The presence of substituents on the phenyl ring will typically affect the nature of a molecule's electronic structure. The following groups were thus added to the phenyl ring in positions *ortho*, *meta,* and *para* to the SF$_3$ group: nominally electron-withdrawing F, Cl, Br, and donating OH, NH$_2$, NHMe and NMe$_2$. More specifically, placing the SF$_3$ group in the 1-position and -CH$_2$OCH$_3$ at 2, *meta* refers to 3, *para* to 4, and *ortho* to 6.

After each substitution, the -CH$_2$OCH$_3$ group was rotated around the C-C$_{aryl}$ bond to search for the minimum-energy structure. The amount of this rotation is defined by the dihedral angle φ(OCCC$_S$) where C$_S$ refers to the C bonded to the sulfur atom. There are several local minima for different values of φ but the global minimum occurs at $\varphi\sim$ -39°, which corresponds to a geometry much like 1B where a O··S chalcogen bond is present. For *o*, *m*, and *p* derivatives, as well as the unsubstituted molecule, there is also a secondary minimum at $\varphi\sim$ -130°, only slightly higher in energy, within 1 kcal/mol of the global minimum. With regard to other local minima, *o* and *p* derivatives differ from *m*. The former molecules, like the unsubstituted one, have another minimum located at $\varphi\sim$170°, some 2-4 kcal/mol higher in energy than the global minimum. These structures are stabilized by a pair of weak H-bonds. One of these involves a methylene proton from the CH$_2$OCH$_3$ group and a fluorine atom. The other H-bond pairs the oxygen atom of the ether group and a phenyl CH which is

meta to the SF$_3$. The latter H-bond is not possible for the *meta*-substituted molecule, so an energy maximum occurs at this value of φ. But most importantly, the global minimum of all these molecules, whether substituted or not, contains the O··S chalcogen bond, and it is this conformation which is considered further.

Some of the salient features of the various substituted molecules are presented in Table 5, along with the unsubstituted molecule 1B. It should perhaps be stated at the outset that most of the substituent effects are rather small. It is clear from the first column that the presence of any substituent, and in any position, shortens the R(O··S) distance within the chalcogen bond. The degree of this contraction is greatest for the *meta*-substituted molecules, but is only slightly sensitive to the nature of the substituent. Considering the *meta*-substituted molecules as an example, the *m*-Br molecule exhibits the shortest R(O··S), and *m*-F the longest. But even here, the changes in this noncovalent bond length amount to less than 7%. The values of E(2) for the O$_{lp}$→σ*(SF) charge transfer follow a similar pattern, in that the largest values are associated with *meta* substitution, with only mild sensitivity to nature of substituent. It is notable that there is a very strong linear correlation between R(O··S) and E(2), with correlation coefficient R^2 =0.991.

Table 5. Energetic (kcal/mol), geometric, and electronic properties of substituted derivatives of 1B.

	R(O··S), Å	E(2)	ρ, au	$\nabla^2\rho$, au	E_{iso}
unsub 1B	2.663	6.66	0.030	0.088	4.96
meta					
F	2.545	11.00	0.033	0.092	5.21
Cl	2.493	13.12	0.036	0.100	5.62
Br	2.486	13.48	0.037	0.102	6.03
OH	2.524	11.91	0.034	0.096	5.36
NH$_2$	2.520	11.87	0.034	0.097	4.15
NHMe	2.511	12.21	0.035	0.099	4.05
NMe$_2$	2.514	12.28	0.035	0.097	3.97
para					
F	2.577	9.71	0.030	0.087	4.81
Cl	2.573	9.85	0.031	0.088	5.18
Br	2.573	9.86	0.031	0.088	5.37
OH	2.587	9.33	0.029	0.085	4.43
NH$_2$	2.601	8.82	0.028	0.083	3.88
NHMe	2.610	7.95	0.028	0.082	3.86
NMe$_2$	2.609	8.57	0.028	0.082	3.74
ortho					
F	2.577	9.52	0.031	0.088	4.66
Cl	2.561	10.1	0.032	0.091	3.78
Br	2.555	10.31	0.033	0.092	3.67
OH	2.582	9.27	0.031	0.088	3.78
NH$_2$	2.552	10.57	0.032	0.092	3.62
NHMe	2.546	10.78	0.033	0.093	3.35
NMe$_2$	2.601	8.64	0.029	0.085	3.24

AIM analysis of the electron density reveals a bond critical point between the oxygen and sulfur atoms in all cases. The value of ρ at this point, as well as its Laplacian, are reported in the next two columns of Table 5. In all cases, ρ is in the 0.028 - 0.037 range, and $\nabla^2\rho$ between 0.082 and 0.102. Both quantities lie in their upper ranges for *meta* substitution.

There is no completely unambiguous means of assessing the energy of an intramolecular interaction. Of the various prescriptions developed for approximating this property, application of an isodesmic reaction should offer a realistic, if imperfect, value. As applied to the systems of interest here, reference is again made to Fig 3 where C contains the full molecule and D only the phenyl ring. A and B each contain one of the two functional groups. The substituent X is included for all four segments. The difference in energy for the reaction A + B → C + D should offer a realistic assessment of the energy of the S··O chalcogen bond which is contained only in C. As indicated in the first row of Table 5, this E_{iso} is equal to 4.96 kcal/mol for the unsubstituted 1B. With respect to the *meta*-substituted molecules, this bond is strengthened for the halogens and OH, and weakened for NH_2, NHMe and NMe_2. The *ortho*-substituted molecules, on the other hand, all exhibit a weaker S··O. Weakening, albeit not quite as much, is also characteristic of the *para*-substituted systems, with the exception of Br and Cl.

In summary, substitution on the aryl ring leads to a modest amount of shortening of the R(O··S) chalcogen bonds, in tandem with increases of the $O_{lp}\rightarrow\sigma^*(S\text{-}F)$ charge transfer contained within E(2). These changes are largest for *m*-substitution. It may be noted that all substituents yield similar trends, at least qualitatively, even though some are generally considered electron-withdrawing and others releasing. On the other hand, all substituents manifest as electron-withdrawing within the context of the full molecules in that all are associated with a partial negative charge. For example, the NH_2 group acquires a charge of -0.10 in this system, even though it is commonly thought of as electron-releasing. And indeed, the AIM parameters in Table 5 show little difference between any of the substituents, also suggesting a chalcogen bond strengthening, albeit a very small one.

CONCLUSIONS

When replacing an fluorine atom of SF_4, there is a strong preference for a phenyl group to occupy one of the equatorial positions. In fact, in the gas phase, there is no minimum in which the phenyl group is in an apical position. Such a minimum occurs in solution, but the apical structure is much higher in energy than the equatorial configuration.

The preference for an equatorial position remains when the phenyl group is substituted with an ether - CH_2OCH_3 group in a position *ortho* to S. The optimal geometry contains an intramolecular O··S chalcogen bond as a major stabilizing force. This same bond occurs as well in the apical geometry, and accounts for its existence as a true minimum of this configuration even in the gas phase. The S··O chalcogen bond occurs also

when both *ortho* positions of the phenyl are occupied by ether groups. This bond appears to be a stronger influence upon the structure than the various CH··F and CH··O H-bonds which it replaces. The apical geometry of this disubstituted molecule contains two O··S chalcogen bonds in its most stable structure.

Placing these systems within a solvent environment does not change any of the above trends. Increasing the polarizability of the solvent leads to a progressive strengthening of the chalcogen bonds. The R(S··O) interatomic distances contract and the NBO value of E(2) is increased. The S-F bond lengthening associated with the formation of the S··O chalcogen bond is enhanced in solution, as are the increases in fluorine atom negative charges. The weakening of these S-F bonds would likely facilitate the catalytic activity of these molecules as deoxofluorinating agents. Solvation also reduces the energetic differences between the apical and equatorial geometries, albeit by only a small amount.

The addition of a second substituent on the phenyl ring, in addition to the ether functionality, has only minor effects on the properties and energetics. All substituents, whether nominally electron-donating or withdrawing, and in any position on the phenyl ring, strengthen the O··S chalcogen bond. This conclusion is supported by a shorter R(S··O) distance and larger value of E(2). AIM quantities offer a slightly different conclusion: greater ρ and $\nabla^2\rho$ at the bond critical point are substantial only for the *meta* positioning of the substituent. As an intramolecular interaction, the energy of the S··O noncovalent bond is difficult to define unambiguously. An isodesmic measure of this property suggests the bond is strengthened when electron-withdrawing substituents, e.g. F or Br, are placed adjacent to the ether, *meta* to SF_3.

While there is little experimental structural information available about these system, it should be noted finally that the computational finding of a trigonal bipyramidal framework is consistent with NMR spectroscopic data.

ACKNOWLEDGMENTS

SUPPORTING INFORMATION

Atomic coordinates and energies of optimized structures. This material is available free of charge via the Internet at http://pubs.acs.org.

REFERENCES

1. Hunter, L. *Beilstein J. Org. Chem.* **2010,** *6*, DOI: 10.3762/bjoc.6.38.
2. Müller, K.; Faeh, C.; Diederich, F. *Science* **2007,** *317*, 1881.
3. McGrath, N. A.; Brichacek, M.; Njardarson, J. T. *J. Chem. Ed.* **2010,** *87*, 1348.
4. Wang, J.; Sánchez-Roselló, M.; Aceña, J. L.; del Pozo, C.; Sorochinsky, A. E.; Fustero, S.; Soloshonok, V. A.; Liu, H. *Chem. Rev.* **2014,** *114*, 2432.
5. Ji, W.-Y.; Xia, X.-L.; Ren, X.-H.; Wang, F.; Wang, H.-J.; Diao, K.-S. *Struct. Chem.* **2013,** *24*, 49.
6. Fried, J.; Mitra, D. K.; Nagarajan, M.; Mehrotra, M. M. *J. Med. Chem.* **1980,** *23*, 234.
7. Rowley, M.; Hallett, D. J.; Goodacre, S.; Moyes, C.; Crawforth, J.; Sparey, T. J.; Patel, S.; Marwood, R.; Patel, S.; Thomas, S.; Hitzel, L.; O'Connor, D.; Szeto, N.; Castro, J. L.; Hutson, P. H.; MacLeod, A. M. *J. Med. Chem.* **2001,** *44*, 1603.
8. Hasek, W. R.; Smith, W. C.; Engelhardt, V. A. *J. Am. Chem. Soc.* **1960,** *82*, 543.
9. Middleton, W. J. *J. Org. Chem.* **1975,** *40*, 574.
10. Lal, G. S.; Pez, G. P.; Pesaresi, R. J.; Prozonic, F. M.; Cheng, H. *J. Org. Chem.* **1999,** *64*, 7048.
11. Yarovenko, N. N.; Raksha, M. A.; Shemanina, V. N.; Vasileva, A. S. *J. Gen. Chem. USSR* **1957,** *27*, 2246.
12. Takaoka, A.; Iwakiri, H.; Ishikawa, N. *Bull. Chem. Soc. Jpn.* **1979,** *52*, 3377.
13. Umemoto, T.; Singh, R. P.; Xu, Y.; Saito, N. *J. Am. Chem. Soc.* **2010,** *132*, 18199.
14. Werz, D. B.; Gleiter, R.; Rominger, F. *J. Am. Chem. Soc.* **2002,** *124*, 10638.
15. Sanz, P.; Yáñez, M.; Mó, O. *Chem. Eur. J.* **2003,** *9*, 4548.
16. Cozzolino, A. F.; Vargas-Baca, I.; Mansour, S.; Mahmoudkhani, A. H. *J. Am. Chem. Soc.* **2005,** *127*, 3184.
17. Gleiter, R.; Werz, D. B.; Rausch, B. J. *Chem. Eur. J.* **2006,** *9*, 2676.
18. Bleiholder, C.; Werz, D. B.; Koppel, H.; Gleiter, R. *J. Am. Chem. Soc.* **2006,** *128*, 2666.
19. Iwaoka, M.; Isozumi, N. *Molecules* **2012,** *17*, 7266.
20. Jablonski, M. *J. Phys. Chem. A* **2012,** *116*, 3753.
21. Zhao, J.-L.; Li, Q.-Z.; Liu, Z.-B.; Li, W.-Z.; Cheng, J.-B. *Mol. Phys.* **2012,** *110*, 2969.
22. Bauzá, A.; Quiñonero, D.; Deyà, P. M.; Frontera, A. *CrystEngComm* **2013,** *15*, 3137.
23. Esrafili, M. D.; Vakili, M. *Mol. Phys.* **2014,** *112*, 2746.
24. Begum, S.; Subramanian, R. *Phys. Chem. Chem. Phys.* **2014,** *16*, 17658.
25. George, J.; Deringer, V. L.; Dronskowski, R. *J. Phys. Chem. A* **2014,** *118*, 3193.
26. Phuong, V. T.; Trang, N. T. T.; Vo, V.; Trung, N. T. *Chem. Phys. Lett.* **2014,** *598*, 75.
27. Azofra, L. M.; Scheiner, S. *J. Chem. Phys.* **2014,** *140*, 034302.
28. Azofra, L. M.; Scheiner, S. *Phys. Chem. Chem. Phys.* **2014,** *16*, 5142.
29. Azofra, L. M.; Scheiner, S. *J. Phys. Chem. A* **2014,** *118*, 3835.
30. Azofra, L. M.; Alkorta, I.; Scheiner, S. *Phys. Chem. Chem. Phys.* **2014,** *16*, 18974.
31. Frisch, M. J.; Trucks, G. W.; Schlegel, H. B.; Scuseria, G. E.; Robb, M. A.; Cheeseman, J. R.; Scalmani, G.; Barone, V.; Mennucci, B.; Petersson, G. A.; Nakatsuji, H.; Caricato, M.; Li, X.; Hratchian, H. P.; Izmaylov, A. F.; Bloino, J.; Zheng, G.; Sonnenberg, J. L.; Hada, M.; Ehara, M.; Toyota, K.; Fukuda, R.; Hasegawa, J.; Ishida, M.; Nakajima, T.; Honda, Y.; Kitao, O.; Nakai, H.; Vreven, T.; Montgomery, J., J. A.; Peralta, J. E.; Ogliaro, F.; Bearpark, M.; Heyd, J. J.; Brothers, E.; Kudin, K. N.; Staroverov, V. N.; Kobayashi, R.; Normand, J.; Raghavachari, K.; Rendell, A.; Burant, J. C.; Iyengar, S. S.; Tomasi, J.; Cossi, M.; Rega, N.; Millam, J. M.; Klene, M.; Knox, J. E.; Cross, J. B.; Bakken, V.; Adamo, C.; Jaramillo, J.; Gomperts, R.; Stratmann, R. E.; Yazyev, O.; Austin, A. J.; Cammi, R.; Pomelli, C.; Ochterski, J. W.; Martin, R. L.; Morokuma, K.; Zakrzewski, V. G.; Voth, G. A.; Salvador, P.; Dannenberg, J. J.; Dapprich, S.; Daniels, A. D.; Farkas, O.; Foresman, J. B.; Ortiz, J. V.; Cioslowski, J.; Fox, D. J. *Gaussian 09*, Revision B.01; Wallingford, CT, 2009.
32. Barone, V.; Cossi, M. *J. Phys. Chem. A* **1998,** *102*, 1995.
33. Reed, A. E.; Curtiss, L. A.; Weinhold, F. *Chem. Rev.* **1988,** *88*, 899.

34. Reed, A. E.; Weinhold, F.; Curtiss, L. A.; Pochatko, D. J. *J. Chem. Phys.* **1986,** *84*, 5687.
35. Bader, R. F. W. *Atoms in Molecules, A Quantum Theory*. Clarendon Press: Oxford, 1990; Vol. 22, p 438.
36. Keith, T. A. *AIMALL*, TK Gristmill Software: Overland Park KS, 2013.
37. Grabowski, S. J. *Chem. Phys. Lett.* **2014,** *605-606*, 131.
38. Scheiner, S. *Acc. Chem. Res.* **2013,** *46*, 280.
39. Alkorta, I.; Elguero, J.; Grabowski, S. J. *Phys. Chem. Chem. Phys.* **2015,** *17*, 3261.
40. Sladek, V.; Škorňa, P.; Poliak, P.; Lukeš, V. *Chem. Phys. Lett.* **2015,** *619*, 7.
41. Solimannejad, M.; Gharabaghi, M.; Scheiner, S. *J. Chem. Phys.* **2011,** *134*, 024312.
42. Sánchez-Sanz, G.; Trujillo, C.; Alkorta, I.; Elguero, J. *Comput. Theor. Chem.* **2015,** *1053*, 305.
43. Adhikari, U.; Scheiner, S. *Chem. Phys. Lett.* **2012,** *532*, 31.
44. Del Bene, J. E.; Alkorta, I.; Elguero, J. *J. Phys. Chem. A* **2014,** *119*, 224.
45. Scheiner, S. *Phys. Chem. Chem. Phys.* **2011,** *13*, 13860.
46. Shahi, A.; Arunan, E. *Phys. Chem. Chem. Phys.* **2014,** *16*, 22935.
47. Scheiner, S. *Int. J. Quantum Chem.* **2013,** *113*, 1609.
48. Scheiner, S. *J. Chem. Phys.* **2011,** *134*, 094315.
49. Nziko, V. d. P. N.; Scheiner, S. *J. Phys. Chem. A* **2014,** *118*, 10849.
50. Sanchez-Sanz, G.; Trujillo, C.; Alkorta, I.; Elguero, J. *Phys. Chem. Chem. Phys.* **2014,** *16*, 15900.

Table of Contents Graphic

intramolecular S---O noncovalent
chalcogen bond

E ~ 5 kcal

2.63 Å

2.71 Å   2.71 Å